forum acusticum 2026
8-12 September · Graz, Austria

ACOUSTIC CLASSIFICATION OF VISUALLY IDENTICAL MATERIALS USING IMPACT EMISSIONS

Anna Maly[1], Stefan Grebien[1], Hannes Bradl[1], Franz Graf[1]

[1] *Joanneum Research Forschungsgesellschaft mbH, Graz, Austria*

This paper is a revised version of the authors' submitted manuscript that was peer-reviewed by at least two anonymous reviewers.

Abstract

Human hearing can reliably distinguish materials based on impact sounds, and machine learning methods can replicate this ability when acoustic differences are pronounced. However, discriminating between materials that sound highly similar even to the human ear remains challenging.

In this study, we demonstrate that glass and metal can be effectively separated using simple thresholding of acoustic features. In contrast, classifying eight types of optically identical plastic parts of identical geometry proves significantly more difficult. For this eight-class task, models trained on 48 kHz signals achieve an accuracy of 25%, exceeding the random baseline of 12.5%. Increasing the sampling rate to 192 kHz improves performance to 36%, while cascading classification strategies further raise accuracy to 47%, with some plastic types exceeding 60% class-wise accuracy. These results show that acoustically distinguishing visually identical plastic materials is feasible with moderate accuracy. The experimental setup ensures that observed signal variations arise solely from intrinsic material properties.

Keywords: *acoustic impact emission, acoustic material characterization, cascaded decision, black plastics*

1. Introduction

Optical material characterization is widely used but can be unreliable for highly reflective materials such as glass or metal, as well as for low-reflectance black plastics. These limitations motivate the investigation of alternative sensing modalities.

Acoustic impact analysis provides a promising alternative, as materials exhibit characteristic vibration and damping behavior when mechanically excited [1]. It has been applied in domains such as food quality assessment, forensics, and waste recycling [2], [3]. Prior work has demonstrated high classification accuracy for tasks involving materials with clearly distinguishable acoustic signatures, often in binary settings [4], [5], [6].

More challenging scenarios arise when materials exhibit similar acoustic behavior. For example, Huang et al. [7] investigated acoustic classification of End-of-Life Vehicle plastics, but their approach relied on limited frequency ranges and varying object geometries, which introduce additional discriminative cues.

In this work, we investigate a significantly more constrained scenario: the acoustic differentiation of visually identical materials with identical geometry. By eliminating shape- and size-related cues, classification must rely solely on intrinsic material properties reflected in the acoustic response. This setup allows us to explore the limits of acoustic material distinguishability.

We first analyze the separability of glass and metal components with similar geometry and show that simple acoustic features enable reliable discrimination and repeatable identification. We then address a more challenging eight-class problem involving black plastics of identical shape and nearly identical mass, where only subtle differences in damping and spectral characteristics are available.

Our contributions are threefold: (i) a controlled experimental setup isolating material-dependent acoustic properties, (ii) an analysis of high-frequency acoustic information for material classification, and (iii) the evaluation of cascading classification strategies to improve robustness in challenging multi-class scenarios.

Due to company policy, the recorded measurement data cannot be made publicly available.

2. Material and Methods

2.1. Material

For the high-reflectance scenario, coated glass (mirror) and aluminum samples were used as test objects (see Fig. 1). The aluminum specimens were obtained from canned corn lids. These materials were selected to evaluate acoustic separability in cases where optical

Corresponding author: *anna.maly@joanneum.at.*

Figure 1: Ten mirror pieces on the left, ten metal pieces on the right

Figure 2: Black Plastics, ABS (Acrylnitril-Butadien-Styrol)

characterization is challenging due to strong surface reflections.

For the low-reflectance scenario, black plastic samples of identical geometry were used to investigate the limits of acoustic material characterization. To ensure high reproducibility, commercially available black plastic welding rods were employed. The rods were cut into segments of 5 mm length with a diameter of 3 mm, resulting in samples of identical size and shape (see Fig. 2). This controlled geometry eliminates shape-related acoustic variations, ensuring that differences in the recorded signals originate primarily from intrinsic material properties.

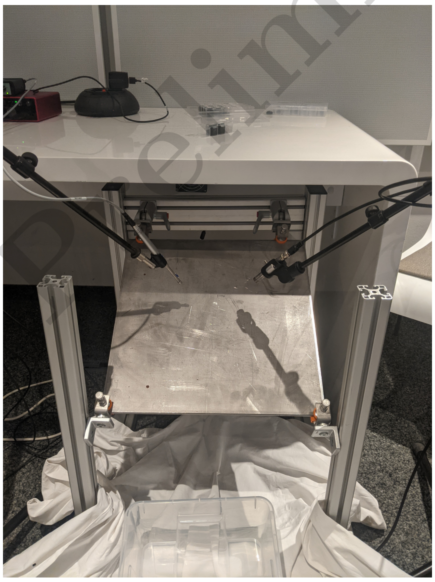

Figure 3: Measurement Setup

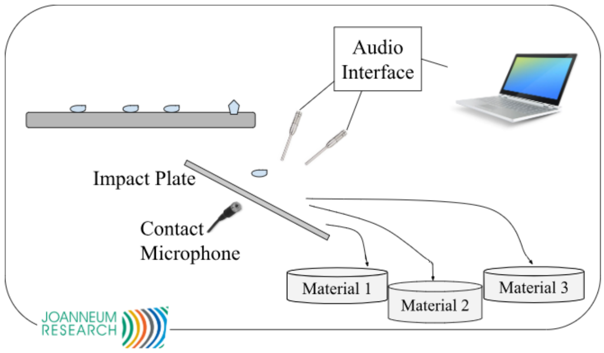

Figure 4: Schematic of experimental aparatus

2.2. Measurement Setup

The experimental setup is shown in Fig. 3, with a schematic representation in Fig. 4. The system consists of a steel impact plate and three microphones for acoustic signal acquisition. Test objects were dropped from a constant height of 27 cm onto the plate.
The steel plate has dimensions of 400 mm × 400 mm × 8 mm and is inclined at 30°. The plate thickness was selected to provide a mechanically rigid and massive impact surface. Owing to the large mass and bending stiffness mismatch between plate and specimen, only a small fraction of the impact energy is converted into plate vibrations, while the dominant resonant response originates from the test object. The inclination ensures sufficient impact energy while preventing the objects from remaining on the surface after impact.
Three microphones were employed: (i) a measurement microphone with a linear response up to 20 kHz, (ii) a wideband measurement microphone with a linear response up to 100 kHz, and (iii) a contact microphone mounted centrally on the underside of the plate. The airborne microphones were positioned 8 cm from the impact location to capture radiated sound, while the contact microphone recorded structure-borne vibrations. The wideband microphone enables detection of high-frequency components beyond the conventional audible range, which may contain material-specific information. Different gain settings were applied to extend dynamic range, following the approach in [4].
All signals were recorded at a sampling rate of 192 kHz, which comfortably covers the usable bandwidth of the microphones up to 100 kHz. The recording start was triggered using a threshold on the contact microphone signal to ensure consistent temporal alignment of impact events. For repeatability analysis, each glass and metal specimen was recorded ten times under identical conditions. The first measurement campaign included ten mirror samples and ten aluminum samples of comparable dimensions (see Fig. 1). Individual object IDs were assigned to enable object-level repeatability evaluation.

2.3. Dataset

The dataset for the high-reflectance classification task is summarized in Table 1, where *Rec. per I.* denotes

Table 1: Dataset high-reflectance. *Rec. p. I.* means recordings per material

Material	Items	Rec. p. I.	Purpose
Glass (Mirror)	10	10	All
Metal (Can Lids)	10	10	All

Table 2: Dataset low-reflectance. Abbreviations in Table 4

Material	Recordings
ABS	824
PA	779
PP	794
PC	879
PPEPDM	758
PEHD	818
PS	787
PVCU	817

the number of recordings per item. The measurements for the low-reflectance case are summarized in Table 3, with the resulting number of valid recordings given in Table 2. The plastic samples were divided into training and test sets, as also indicated in Table 3. This ensures a strict generalization setting, where the model must learn material-specific characteristics rather than object-specific patterns.

3. Theory and Calculation

3.1. Acoustic Impact Emission

An impact event excites the resonant modes of an object, which are reflected in its time–frequency representation. In this work, excitation is approximated by dropping objects onto a rigid plate, generating a broadband impulse.

The resulting acoustic response is governed by material properties (e.g., density and elastic moduli) and geometry. While geometry influences the exact resonance frequencies, identical shapes constrain these variations, such that remaining differences primarily reflect intrinsic material properties. Due to the small size of the samples (millimeter scale), relevant spectral content extends beyond 20 kHz. Therefore, signals are recorded at 192 kHz to capture high-frequency components.

Table 3: Measurements for low-reflectance materials. *Rec. p. Mat.* means recordings per material

Date	Rec. p. Mat.	Purpose	Set
02 - 20	~330 (2778)	triple drop	Train
02 - 21	~190 (1592)	5 x drop, obj IDs	Test
07 - 31	~110 (886)	single drop	Train
07 - 31	30 (240)	3 x drop, obj IDs	Test
08 - 01	20 (160)	single drop	Test
08 - 01	20 (160)	single drop	Train
08 - 02	~87 (693)	single drop	Train

Table 4: Abbreviations of plastic items

Abbrev.	Code	Material
ABS	pla_abs	Acrylnitril-Butadien-Styrol
PA	pla_pa	Polyamid
PP	pla_pp	Polypropylen
PC	pla_pc	Polycarbonat
PPEPDM	pla_ppepdm	Polypropylen/ Ethylen-Propylen-Dien-Monomer
PEHD	pla_hdpe	Polyethylen high density
PS	pla_ps	Polystyrol
PVCU	pla_pvcu	Polyvinylchlorid hard

3.2. Repeatability

Although impact conditions vary (e.g., orientation and contact point), the resonant characteristics remain stable. Repeatability is assessed using repeated measurements of identical samples.

3.3. Machine Learning Methods

Given the limited dataset size, classical machine learning methods were employed. In particular, support vector machines (SVMs) are used due to their robustness and interpretability. Model details are provided in Section 4.2.

3.4. Cascading

Single impacts may not fully excite all relevant modes due to variations in impact conditions. To improve robustness, multiple measurements of the same object are aggregated. For each object, class probabilities are combined by taking the median across repetitions, and the final class is determined by the maximum aggregated probability. This approach reduces the influence of outliers and improves classification performance.

4. Results

4.1. Highly reflective items: Glass and metal

Representative spectrograms of metal and glass samples are shown in Fig. 5. The spectrograms are time-aligned with respect to the impact event, and their amplitudes are normalized to a maximum of 1 (0 dB). Distinct differences between the two material classes can be observed. Metal samples exhibit sustained energy at discrete frequencies over time, visible as horizontal structures in the spectrogram. In contrast, glass samples show a more broadband response, with energy distributed across a wider frequency range and stronger temporal variation.

Even simple statistical features allow reliable discrimination between the two materials. Fig. 6 shows the standard deviation of a representative frequency bin at 2625 Hz over a time window from impact to 20 ms after impact. This frequency bin was selected as representative due to its strong discriminative behavior across classes. The Short-Time Fourier Transform (STFT) was computed using a sampling rate of 192 kHz, a window size of 512 samples, and an overlap of 448 samples, resulting in 257 frequency bins and 60 time

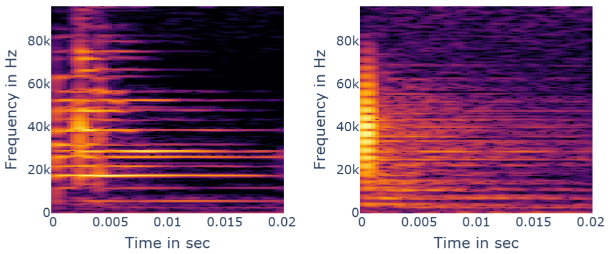

Figure 5: Representative spectrograms of metal (left) and glass (right)

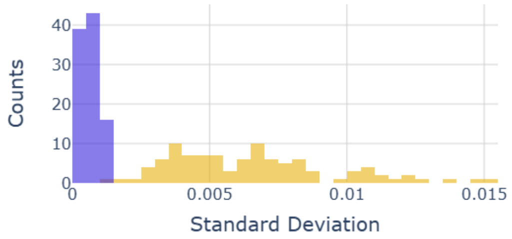

Figure 6: Histogram of a frequency bin standard deviations

frames. Next, the reproducibility of the generated signals was analyzed. Fig. 7 shows spectrograms of four impact measurements of the same metal sample, computed using a Short-Time Fourier Transform. The same characteristic frequencies are consistently excited across all measurements. However, variations in impact conditions, such as differences in orientation or contact point, lead to changes in the amplitudes of the excited modes. Fig. 8 shows spectrograms of a different metal sample. In comparison, distinct frequency patterns can be observed, indicating that each object exhibits a characteristic acoustic fingerprint.
Due to the limited number of measurements and the clear separability of the samples, machine learning methods were not applied for this classification task.

4.2. Weakly reflective items: Black plastics

The classification of the plastic samples represents a significantly more challenging task. The time–frequency spectrograms appear highly similar, making them difficult to distinguish even for human listeners [8], and conventional features show little separability. Therefore, this scenario can be considered close to the limits of acoustic material discrimination. Nevertheless, meaningful classification performance can still be achieved.
To reduce overfitting and improve generalization, the data was collected across multiple recording sessions on different days. While key components of the setup (measurement environment, sensors, sound cards, and impact plate) remained unchanged, variations in temperature, operator position, and microphone placement were present.

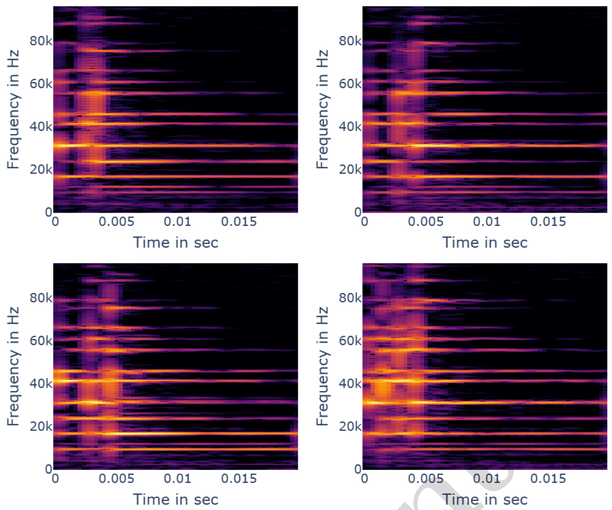

Figure 7: Time-frequency-spectrograms of four measurements of the same metal item (ID 10).

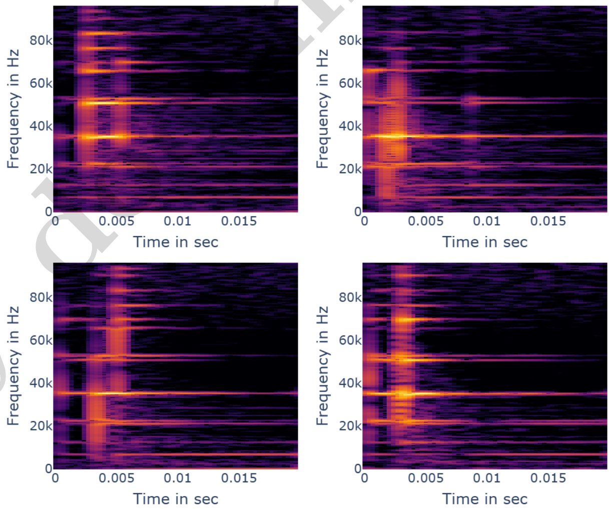

Figure 8: Time-frequency-spectrograms of four measurements of the same metal item (ID 6).

The test data was drawn from different measurement sessions than the training data (see Table 3). In addition, the plastic samples used for training and testing were distinct, ensuring object-level separation between both sets.

4.2.1. Used Audio Data and Features

A threshold on the contact microphone signal is used to detect impact events. For each event, an audio segment from the wideband microphone is extracted, starting 1 ms before the threshold crossing and spanning 21 ms, sampled at 192 kHz. Mel power spectrograms with 41 Mel bands are computed using Hann windows of 800 samples with an overlap of 768 samples. After discarding the first Mel band, each spectrogram results in 3744 features. Dimensionality reduction is performed using principal component analysis (PCA),

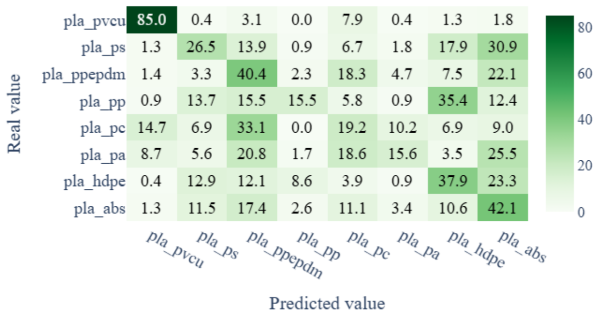

Figure 9: Confusion matrix of test set in %; accuracy: 35.7%; for material designation see Table 4

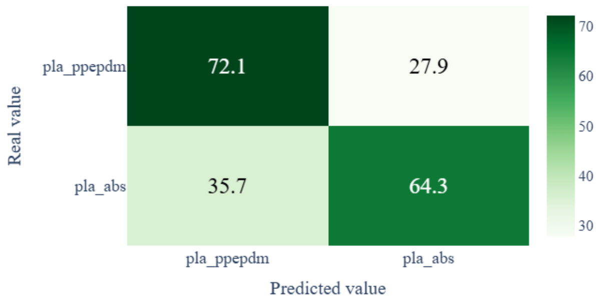

Figure 12: Two-Class-Confusion matrix of test set in %; accuracy: 68%; for material designation see Table 4

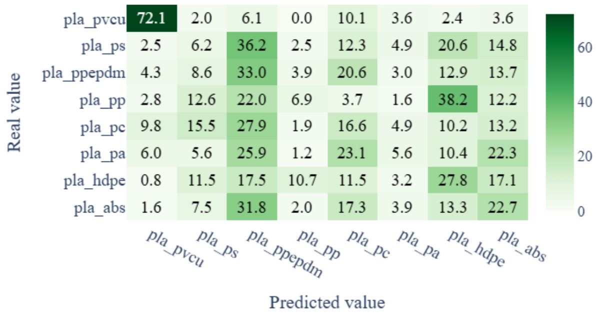

Figure 10: Confusion matrix of $48kHz$ test set in %; accuracy: 24.5%; for material designation see Table 4

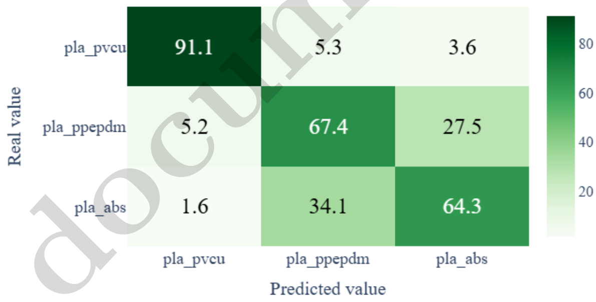

Figure 13: Three-Class-Confusion matrix of test set in %; accuracy: 74.4%; for material designation see Table 4

retaining the first 200 principal components.

4.2.2. Machine Learning Method

A support vector machine (SVM) with hyperparameters selected based on validation performance was used for classification. A one-vs-one scheme was applied for multi-class classification, and all features were standardized prior to training. Training was performed using all recordings of the training item set, while all recordings of the test item set were used for evaluation. This setup yields an overall classification accuracy of 35%. The corresponding confusion matrix is shown in Fig. 9. For comparison, reducing the sampling rate to 48 kHz decreases the accuracy to 24.5%, highlighting the importance of high-frequency information. When restricting the classification to subsets of classes, performance improves. Results for two-class and three-class scenarios are shown in Fig. 11, Fig. 12, and Fig. 13. We also evaluated neural network models, but they achieved lower performance ($\approx$ 30% accuracy) than the SVM ($\approx$ 36% accuracy), likely due to the limited dataset size.

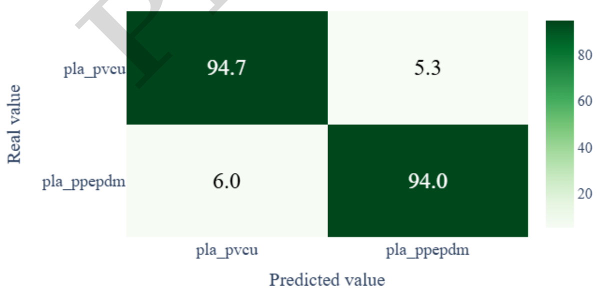

Figure 11: Two-class-confusion matrix of test set in %; accuracy: 94.8%; for material designation see Table 4

4.2.3. Cascading

For the cascading approach, multiple impact measurements were recorded for each test sample, with consistent object IDs assigned across repetitions. The trained SVM model was used to obtain class probability estimates for each individual recording. For each object, the predicted class probabilities were aggregated across all associated recordings by computing the median per class. The final class label was then determined by selecting the class with the highest

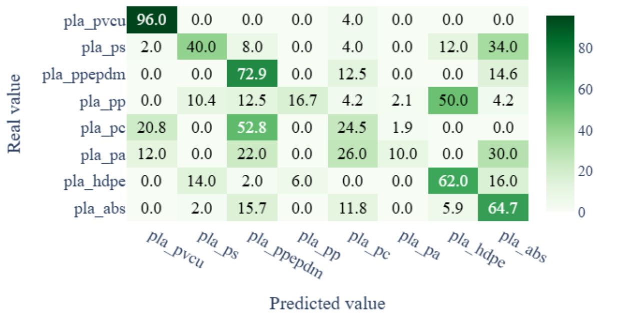

Figure 14: Confusion matrix of cascaded test set in %; accuracy: 47.0%; for material designation see Table 4

median probability. This aggregation improves robustness and increases the overall classification accuracy to 47 %, as shown in Fig. 14. This represents a substantial relative improvement of approximately 34 %, highlighting the effectiveness of aggregating multiple impact measurements in reducing variability.

5. Discussion and Conclusion

This work investigated the limits of acoustic material classification for visually identical objects with identical geometry, thereby isolating intrinsic material-dependent acoustic properties.

The results demonstrate that materials with distinct acoustic signatures can be reliably classified, while discrimination between acoustically similar materials remains challenging but feasible. A key finding is the importance of high-frequency information: increasing the sampling rate from 48 kHz to 192 kHz improves classification accuracy by 11 percentage points, indicating that relevant material-specific information is contained beyond the conventional audible range.

Classification performance strongly depends on the task complexity. While selected two-class problems achieve high accuracy (e.g., 94.8% for PVC-U vs. PPEPDM), the full eight-class problem remains difficult due to the high similarity of the acoustic responses. Aggregating multiple measurements using a cascading strategy significantly improves robustness, highlighting the importance of mitigating variability in impact conditions.

The proposed approach offers a low-cost and efficient solution suitable for embedded systems. However, it requires controlled conditions, including consistent object geometry, stable measurement setups, and representative training data. In particular, geometric variations would introduce additional spectral cues and alter the classification problem.

Overall, acoustic impact emission analysis is a promising alternative to optical material characterization, especially in scenarios where optical methods are limited. Future work will focus on improving robustness under less controlled conditions, analyzing the role of high-frequency features in more detail, and extending the method to additional materials and applications.

6. Acknowledgment

This research was funded by the Federal Ministry of the Republic of Austria, responsible for Climate Action, Environment, Energy, Mobility, Innovation and Technology.

References

[1] B. L. Giordano and S. McAdams, “Material identification of real impact sounds: Effects of size variation in steel, glass, wood, and plexiglass plates,” *The Journal of the Acoustical Society of America*, vol. 119, no. 2, pp. 1171–1181, 2006.

[2] M. Guo, Y. Ma, X. Yang, and R. W. Mankin, “Detection of damaged wheat kernels using an impact acoustic signal processing technique based on gaussian modelling and an improved extreme learning machine algorithm,” *biosystems engineering*, vol. 184, pp. 37–44, 2019.

[3] G. Maier, R. Gruna, T. Längle, and J. Beyerer, “A survey of the state of the art in sensor-based sorting technology and research,” *IEEE Access*, 2024.

[4] T. C. Pearson, A. E. Cetin, A. H. Tewfik, and R. P. Haff, “Feasibility of impact-acoustic emissions for detection of damaged wheat kernels,” *Digital Signal Processing*, vol. 17, no. 3, pp. 617–633, 2007.

[5] H. Kalkan, N. F. Ince, A. H. Tewfik, Y. Yardimci, and T. Pearson, “Classification of hazelnut kernels by using impact acoustic time-frequency patterns,” *EURASIP Journal on Advances in Signal Processing*, vol. 2008, pp. 1–11, 2007.

[6] M. Omid, “Design of an expert system for sorting pistachio nuts through decision tree and fuzzy logic classifier,” *Expert Systems with Applications*, vol. 38, no. 4, pp. 4339–4347, 2011.

[7] J. Huang, C. Tian, J. Ren, and Z. Bian, “Study on impact acoustic—Visual sensor-based sorting of ELV plastic materials,” *Sensors*, vol. 17, no. 6, p. 1325, 2017.

[8] G. Lemaitre and L. M. Heller, “Auditory perception of material is fragile while action is strikingly robust,” *The Journal of the Acoustical Society of America*, vol. 131, no. 2, pp. 1337–1348, 2012.